Received: 9 July 2023 | Revised: 22 September 2023 | Accepted: 25 September 2023

DOI: 10.1002/pamm.202300282

RESEARCH ARTICLE

A large strain thermoplasticity model including recovery, recrystallisation and grain size effects

Merlin Böddecker[1] | **Andreas Menzel**[1,2]

[1]Institute of Mechanics, TU Dortmund University, Dortmund, Germany

[2]Division of Solid Mechanics, Lund University, Lund, Sweden

Correspondence
Merlin Böddecker, Institute of Mechanics, TU Dortmund University, Leonhard-Euler-Str. 5, 44227 Dortmund, Germany.
Email: merlin.boeddecker@tu-dortmund.de

Funding information
Deutsche Forschungsgemeinschaft, Grant/Award Number: 278868966

Abstract

In manufacturing, thermomechanical processes such as static annealing and hot working are commonly used to tailor the microstructure of metals to achieve favourable macroscopic material properties that meet specific application requirements. To improve sequential manufacturing processes and to accurately predict the microstructural changes of the material along the process chain, physically motivated constitutive models are required that simultaneously account for the effects of recovery and recrystallisation, as well as grain size dependencies. To this end, Cho et al. [Int. J. Plasticity **112**, 123–157 (2019)] proposed a macroscopic hypo-elasticity based large strain thermoplasticity model that aims at the unification of the effects of static and dynamic recovery and recrystallisation, as well as grain growth and refinement. In the present contribution, the hypo-elasticity based large strain recrystallisation formulation proposed by Cho et al. is transferred to a hyper-elasticity based large strain thermoplasticity framework to overcome the limitations typically accompanied with hypo-elasticity based formulations. For this purpose, an isotropic temperature dependent hyper-elastic Hencky type formulation defined in logarithmic strains is combined with a temperature dependent von Mises yield criterion. The recrystallisation modelling approach by Cho et al. is adopted, assuming a non-associated temperature dependent proportional hardening rate in the form of an Armstrong-Frederick type hardening minus recovery format, wherein the proportional hardening related internal variable is interpreted as a measure of dislocation density. It is shown that the hyper-elasticity based format results in a thermodynamical consistency condition that effectively constrains the physically motivated evolutions of recrystallised volume fraction and average grain size. To investigate the capability of the model to predict the material response of unified recrystallisation thermodynamically consistently, representative thermomechanical sequential loading conditions including static annealing and hot working are studied.

1 | INTRODUCTION

In a plastically deforming material, the generation of new dislocations by work hardening leads to the accumulation of hardening related energy contributions represented by an increased dislocation density. At elevated temperatures, the dislocation density acts as a driving force for the initiation of microstructural processes of recovery, recrystallisation and grain size evolution [1, 2]. Recovery, the predecessor to recrystallisation, reduces the dislocation density by annihilation and rearrangement of dislocations, resulting in the formation of low angle grain boundaries. With increasing temperature, plastically deformed grains are replaced with new high angle dislocation free grains by recrystallisation. Both processes of recovery and recrystallisation effectively release the hardening related energy contributions, resulting in a decrease in strength and a simultaneous increase in ductility observed in the macroscopic material response, which will be referred to as the softening effect in the following. Grain growth, the successor to recrystallisation, is driven by grain boundary energy and influences the macroscopic material behaviour in terms of the Hall-Petch effect [3, 4].

In this work, following Cho et al. [5], the two primary underlying recrystallisation mechanisms of subgrain rotation recrystallisation and grain boundary migration recrystallisation are considered, which are both driven by hardening related energy contributions. Subgrain rotation recrystallisation occurs exclusively during plastic loading, that is hot working processes, where new high angle grains form in plastically deformed grains from dislocation walls generated by dynamic recovery [6]. In turn, grain boundary migration recrystallisation is a time dependent recrystallisation mechanism that is observed during both, static annealing and hot working processes. It involves the nucleation and growth of new high angle grains at the grain boundaries, consuming plastically deformed grains [7].

In the literature, several recrystallisation models can be found that are typically limited to specific thermomechanical conditions, focusing on simulating either static recrystallisation, see for example [8, 9], or dynamic recrystallisation, see for example [10–13]. These models commonly adopt a purely phenomenological Avrami type formulation [14, 15] or are based on a physically motivated recrystallised volume fraction evolution that is coupled to hardening related energy contributions. They may depend on a critical value for the onset of recrystallisation or are missing a grain size evolution equation. Other models aim at the unification of the effects of work hardening, recovery, recrystallisation and grain size evolution, see for example [5, 16–18]. However, these models may lack certain model features, such as a coupling to plasticity including the grain size related Hall-Petch effect [3, 4] or are following a hypo-elasticity based formulation.

The unified recrystallisation framework proposed by Cho et al. [5] is based on a hypo-elasticity based large strain thermoplasticity formulation and features physically motivated evolution equations of newly introduced internal state variables of recrystallised dislocation free volume fraction and average grain size. By incorporating a plasticity formulation with the proportional hardening internal variable interpreted as a measure of dislocation density, the evolutions of these internal variables are accurately modelled based on their true physical driving forces of hardening related energy contributions and grain boundary energy. By entering a proportional hardening rate in the form of a hardening minus recovery format by Armstrong and Frederick [19], the recrystallised volume fraction and average grain size internal variables model the microstructure dependent softening and grain size related Hall-Petch effect [3, 4]. In addition, the proposed recrystallisation formulation avoids a critical value for the onset of recrystallisation by employing Arrhenius type functions for the activation of recovery, recrystallisation and grain size evolutions.

As this work proceeds, the hypo-elasticity based thermoplasticity recrystallisation model proposed by Cho et al. [5] is transferred to an isotropic Hencky type hyper-elasticity based thermoplasticity framework to overcome the limitations typically accompanied with hypo-elasticity based formulations. Such hypo-elastic formulations do not define a thermodynamic potential and therefore cannot be proven to adhere to the second law of thermodynamics. As a result, they may lead to unphysical dissipation in the simulation of only elastic processes. Following a hyper-elasticity based framework, a temperature dependent Helmholtz energy function defined in logarithmic strains is introduced as the thermodynamic potential for the underlying constitutive model. Based on a temperature dependent von Mises plasticity, an associated plastic flow rule and a non-associated proportional hardening rate are employed by introducing additional recrystallisation related plastic potentials that follow the hardening minus recovery recrystallisation formulation proposed by Cho et al. [5]. It is shown that the thermodynamical consistent framework results in a thermodynamical consistency condition which gives rise to the thermodynamical intercorrelation between the internal variables of recrystallised volume fraction and average grain size.

2 | A HYPER-ELASTICITY BASED UNIFIED RECRYSTALLISATION MODEL

In a large strain setting, let the motion of a deformable continuum body be defined by $\boldsymbol{x} = \boldsymbol{\varphi}(\boldsymbol{X}, t)$, which is a nonlinear mapping of referential material point placements $\boldsymbol{X} \in \mathcal{B}_0$ to their spatial counterparts $\boldsymbol{x} \in \mathcal{B}_t$ at time $t \in \mathbb{R}$. The related deformation gradient $\boldsymbol{F} = \nabla_{\boldsymbol{X}} \boldsymbol{\varphi}(\boldsymbol{X}, t)$, with $J = det\,(\boldsymbol{F}) > 0$, transforms infinitesimal referential line elements $\mathrm{d}\boldsymbol{X}$ to their spatial counterparts $\mathrm{d}\boldsymbol{x}$. By introducing a locally incompatible and stress-free intermediate configuration, the deformation gradient is assumed to multiplicatively decompose into an elastic part $\boldsymbol{F}_\mathrm{e}$ and a plasticity related internal state variable contribution $\boldsymbol{F}_\mathrm{p}$, so that $\boldsymbol{F} = \boldsymbol{F}_\mathrm{e} \cdot \boldsymbol{F}_\mathrm{p}$, with $J_\mathrm{e} = det\,(\boldsymbol{F}_\mathrm{e}) > 0$.

Based on these definitions, the elastic left Cauchy-Green deformation tensor $\boldsymbol{b}_\mathrm{e} = \boldsymbol{F}_\mathrm{e} \cdot \boldsymbol{F}_\mathrm{e}^\mathrm{t}$ is introduced, wherein $\bullet^\mathrm{t}$ denotes transposition. It gives raise to the elastic logarithmic strain tensor, that is the elastic Hencky strain tensor [20], defined as

$$\boldsymbol{\varepsilon}_\mathrm{e} = \frac{1}{2} \ln(\boldsymbol{b}_\mathrm{e}) = \boldsymbol{\varepsilon}_\mathrm{e}^\mathrm{vol} + \boldsymbol{\varepsilon}_\mathrm{e}^\mathrm{iso}\,, \tag{1}$$

with $\boldsymbol{\varepsilon}_\mathrm{e}^\mathrm{vol} = 1/3\,\mathrm{tr}(\boldsymbol{\varepsilon}_\mathrm{e})\,\boldsymbol{I}$ the volumetric elastic logarithmic strains and $\boldsymbol{I}$ the second-order identity tensor.

A temperature dependent isotropic Helmholtz energy function Ψ defined in elastic logarithmic strains is used for the underlying hyper-elasticity based constitutive framework. To be specific, the Helmholtz energy is assumed to decompose additively into an elastic volumetric, elastic isochoric, thermal and a proportional hardening related plastic contribution, namely

$$\Psi\,(\boldsymbol{b}_\mathrm{e}, \theta, \alpha) = \frac{1}{2} K\,(\theta)\ \mathrm{tr}^2\,(\boldsymbol{\varepsilon}_\mathrm{e}) + G\,(\theta)\ \mathrm{tr}\,\left(\boldsymbol{\varepsilon}_\mathrm{e}^\mathrm{iso} \cdot \boldsymbol{\varepsilon}_\mathrm{e}^\mathrm{iso}\right) + \bar{c}_0\,\left[\theta - \theta_0 - \theta\,\ln\left(\frac{\theta}{\theta_0}\right)\right] + \frac{1}{2} H\,(\theta)\ \alpha^2\,, \tag{2}$$

with α an internal state variable associated with proportional hardening and interpreted as a measure of dislocation density, K and G the temperature dependent compression and shear moduli, $\bar{c}_0$ a heat capacity parameter, $\theta > 0$ the absolute temperature, θ_0 the reference temperature and H the temperature dependent proportional hardening modulus.

Following a hyper-elasticity based format, the mechanical dissipation inequality in local form reads

$$\mathcal{D}_\mathrm{mech} = \boldsymbol{m}^\mathrm{t} : \boldsymbol{l} - \dot{\Psi} \geq 0\,, \tag{3}$$

wherein $\boldsymbol{l} = \nabla_{\boldsymbol{x}} \dot{\boldsymbol{\varphi}}$ is the spatial velocity gradient and $\dot{\bullet} = (\mathrm{d}_t \bullet)|_{\boldsymbol{X}}$ denotes the material time derivative. The spatial Mandel type stresses $\boldsymbol{m}^\mathrm{t}$ are related to the Kirchhoff stresses $\boldsymbol{\tau}$ via $\boldsymbol{m}^\mathrm{t} = \boldsymbol{g} \cdot \boldsymbol{\tau}$, with $\boldsymbol{g}$ the spatial co-variant metric tensor.

Applying the standard Colemann-Noll [21] procedure results in constitutive constraints on the plasticity related thermodynamic driving force $\boldsymbol{m}^\mathrm{t}$, that is Mandel type stresses, and the proportional hardening related thermodynamic driving force β, that is hardening stress, of the form

$$\boldsymbol{m}^\mathrm{t} = 2\,\frac{\partial \Psi}{\partial \boldsymbol{b}_\mathrm{e}} \cdot \boldsymbol{b}_\mathrm{e} = K\,(\theta)\ \mathrm{tr}\,(\boldsymbol{\varepsilon}_\mathrm{e})\ \boldsymbol{I} + 2\,G\,(\theta)\ \boldsymbol{\varepsilon}_\mathrm{e}^\mathrm{iso}\,, \quad \beta = \frac{\partial \Psi}{\partial \alpha} = H\,(\theta)\ \alpha\,. \tag{4}$$

In addition, it can be shown that the heat capacity for transient heat transfer is constrained by $c_0 = -\theta\,\partial^2_{\theta^2} \Psi$. Inserting the above constraints into the dissipation inequality (3) together with the additive split of $\boldsymbol{l} = \boldsymbol{l}_\mathrm{e} + \boldsymbol{l}_\mathrm{p}$ with $\boldsymbol{l}_\mathrm{p} = \boldsymbol{F}_\mathrm{e} \cdot \dot{\boldsymbol{F}}_\mathrm{p} \cdot \boldsymbol{F}^{-1}$, results in the reduced mechanical dissipation inequality

$$\mathcal{D}_\mathrm{mech}^\mathrm{red} = \boldsymbol{m}^\mathrm{t} : \boldsymbol{l}_\mathrm{p} - \beta\,\dot{\alpha} \geq 0\,. \tag{5}$$

As this work proceeds, a rate independent von Mises yield criterion with proportional hardening of type

$$\Phi\,(\boldsymbol{m}^\mathrm{t}, \theta, \beta) = \sqrt{\frac{3}{2}} \|\boldsymbol{m}^\mathrm{tdev}\| - \left[\sigma_{y0}\,(\theta) + \beta\right] \tag{6}$$

is assumed, with $\boldsymbol{m}^\mathrm{tdev} = \boldsymbol{m}^\mathrm{t} - 1/3\,\mathrm{tr}(\boldsymbol{m}^\mathrm{t})\,\boldsymbol{I}$ the deviatoric Mandel type stresses, σ_{y0} the temperature dependent initial yield limit and $\|\bullet\| = \sqrt{\bullet : \bullet}$ denoting the Frobenius norm.

The associated evolution for plasticity related deformation contributions is obtained by enforcing the postulate of maximum dissipation with respect to an admissible plastic domain of $\bar{\mathbb{E}} := \{\boldsymbol{m}^{\mathrm{t}}, \beta \mid \Phi(\boldsymbol{m}^{\mathrm{t}}, \theta, \beta) \leq 0\}$, so that

$$\boldsymbol{l}_{\mathrm{p}} = \lambda \frac{\partial \Phi\left(\boldsymbol{m}^{\mathrm{t}}, \theta, \beta\right)}{\partial \boldsymbol{m}^{\mathrm{t}}} = \lambda \sqrt{\frac{3}{2}} \frac{\boldsymbol{m}^{\mathrm{tdev}}}{\|\boldsymbol{m}^{\mathrm{tdev}}\|}, \tag{7}$$

together with the complementary Karush-Kuhn-Tucker (KKT) conditions of $\Phi \leq 0$, $\lambda \geq 0$ and $\lambda\, \Phi = 0$.

In order to unify the effects of recovery, recrystallisation and grain size, a non-associated proportional hardening variable evolution in terms of plastic loading related (d: dynamic) and time dependent (s: static) plastic potentials $\Phi_{\mathrm{d}}^{\#}$ and $\Phi_{\mathrm{s}}^{\#}$ is assumed to take the form

$$\dot{\alpha} = -\lambda \frac{\partial \Phi_{\mathrm{d}}^{\#}\left(\theta, \beta, X, d_{\mathrm{g}}\right)}{\partial \beta} - \frac{\partial \Phi_{\mathrm{s}}^{\#}\left(\theta, \beta, d_{\mathrm{g}}\right)}{\partial \beta}. \tag{8}$$

Following the recrystallisation modelling approach by Cho et al. [5], the non-associated hardening rate takes a hardening minus recovery format proposed by Armstrong and Frederick [19]. Cho et al. [5] further extended this formulation by influences of newly introduced internal state variables of recrystallised dislocation free volume fraction X, restricted by $0 \leq X \leq 1$, and average grain size d_{g}, representing the microstructure of the material. The proportional hardening evolution equation reads

$$\dot{\alpha}\left(\theta, \lambda, \beta, X, d_{\mathrm{g}}\right) = \left[\lambda\, [1 - X] - \left[\sqrt{\frac{2}{3}}\, R_{\mathrm{d}}\left(\theta\right)\, \lambda + R_{\mathrm{s}}\left(\theta\right)\right] \frac{\beta^2}{H\left(\theta\right)}\right] \left[\frac{d_{\mathrm{g0}}}{d_{\mathrm{g}}}\right]^{z}. \tag{9}$$

Therein, proportional hardening is modelled as a competition between an increase rate and a decrease rate under hot working conditions. The decrease rate takes the form of recovery activated softening of $\sqrt{2/3}\, R_{\mathrm{d}}\, \lambda + R_{\mathrm{s}}$. It is driven by the hardening stress squared divided by the proportional hardening modulus, that is β^2/H, representing hardening related energy contributions. Temperature dependent Arrhenius type activation functions R_{d} and R_{s} of the form

$$R_{\mathrm{d}}(\theta) = C_{13} \exp\left(-\frac{C_{14}}{R\,\theta}\right) \quad \text{and} \quad R_{\mathrm{s}}(\theta) = C_{17} \exp\left(-\frac{C_{18}}{R\,\theta}\right) \tag{10}$$

are used for activation of recovery, where C_{13} and C_{17} are dynamic and static recovery material parameters, C_{14} and C_{18} are dynamic and static recovery activation energies and R is the universal gas constant. The Lagrange multiplier λ distinguishes between plastic loading related (d: dynamic) and time dependent (s: static) recovery contributions. As a result, both recovery mechanisms are active during hot working. Under static annealing conditions, only static recovery becomes active, and a decreasing proportional hardening variable is modelled. The proportional hardening variable increase rate is modelled as a linear contribution of work hardening weighted by the recrystallised volume fraction, that is $\lambda\, [1 - X]$. Based on the precursor of recovery, recrystallisation further increases the softening effect by reducing the work hardening related contribution.

To account for the grain size related Hall-Petch effect [3, 4], the hardening relation (9) is additionally weighted by a factor of $[d_{\mathrm{g}}/d_{\mathrm{g0}}]^{z}$, where d_{g0} is the initial average grain size and z is a grain size material parameter. In the case of cold working with approximately vanishing activation functions $R_{\mathrm{d}} \approx 0$ and $R_{\mathrm{s}} \approx 0$, the hardening relation (9) reduces to a work hardening related contribution weighted by recrystallised volume fraction and the grain size factor. In that way, the influence of the microstructural evolution on cold working processes resulting from preceded, for example, thermal steps is taken into account.

Due to this nonlinear hardening formulation, cf. (9), it is ensured that the proportional hardening variable itself cannot become negative, that is $\alpha \geq 0$, assuming an initial value of $\alpha|_{t_0} \geq 0$, although negative evolutions $\dot{\alpha} < 0$ are possible for a non-vanishing proportional hardening variable.

Following the same format, the recrystallised dislocation free volume fraction evolution is assumed by Cho et al. [5] as a competition between an increase rate and a reduction rate under hot working conditions, that is

$$\dot{X}\left(\theta, \lambda, \beta, X\right) = X^{a}\, [1 - X]^{b}\, \left[C_{\mathrm{xd}}\left(\theta\right)\, \lambda + C_{\mathrm{xs}}\left(\theta\right)\right] \frac{\beta^2}{G\left(\theta\right)} - c_{\mathrm{x5}}\, \frac{H\left(\theta\right)}{G\left(\theta\right)}\, \dot{\alpha}^{*}\, X^{c}, \tag{11}$$

wherein a and b are material parameters related to the interface between recrystallised and non-recrystallised grains, $\dot{\alpha}^* = \dot{\alpha}(\theta, \lambda, \beta, X = 0, d_g = d_{g0})$ is the proportional hardening rate for a virgin material, cf. (9), and c_{x5} and c are reduction rate material parameters.

The recrystallisation increase rate is physically motivated by the replacement of deformed grains with new high angle dislocation free grains and is driven by the squared hardening stress divided by the shear modulus, that is $\beta^2/G(\theta)$. A nonlinear sigmoidal form [2] is employed that is in agreement with experimental results. The Lagrange multiplier distinguishes between plastic loading and time dependent recrystallisation mechanisms related to subgrain rotation recrystallisation and grain boundary migration recrystallisation. The related Arrhenius type activation functions C_{xd} and C_{xs} are defined as

$$C_{xd}(\theta) = c_{x1}\, \exp\left(-\frac{c_{x2}}{R\,\theta}\right) \quad \text{and} \quad C_{xs}(\theta) = c_{x3}\, \exp\left(-\frac{c_{x4}}{R\,\theta}\right), \tag{12}$$

where c_{x1} and c_{x3} are dynamic and static recrystallisation material parameters and c_{x2} and c_{x4} are dynamic and static activation energies for recrystallisation. The recrystallised volume fraction decrease rate, in turn, is associated with the generation of new dislocations by work hardening as a result of plastic loading, cf. (11). For static annealing processes, recrystallised volume fraction increases and for cold working processes only the decrease rate of recrystallised volume fraction is activated, which is in agreement with the expected physical phenomena.

Finally, under hot working conditions, the average grain size evolution is modelled by Cho et al. [5] as a competition between average grain size growth rate and average grain size reduction rate, taking the form

$$\dot{d}_g\left(\theta, \lambda, \beta, X, d_g\right) = \frac{\omega(\theta)}{n\, d_g^{n-1}} - c_{g3}\, \dot{X}_d\, d_g \left[d_s(\theta, \lambda) - d_g\right]^2, \quad \text{with} \quad \dot{X}_d = X^a \left[1 - X\right]^b C_{xd}(\theta)\, \lambda\, \frac{\beta^2}{G(\theta)}, \tag{13}$$

where n is the parabolic curvature exponent, c_{g3} is the grain size reduction rate material parameter, $\dot{X}_d$ is the plastic loading related recrystallised volume fraction increase rate extracted from (11), and d_s is the steady state average grain size. The average grain size growth rate is driven by the grain boundary energy and is temperature activated by an Arrhenius type function $\omega(\theta) = \omega_0 \exp(-E^*/[R\,\theta])$ with ω_0 the grain size growth rate material parameter and E^* the activation energy for grain size growth. An average grain size growth driven by hardening related energy contributions is not included in Cho et al. [5] and remains for future work.

In contrast, the average grain size reduction rate is assumed to be mainly associated with dynamic recrystallisation under plastic loading and is bounded below by the condition $d_g \geq d_s$ with the temperature dependent steady state average grain size defined as

$$d_s(\theta, \lambda) = c_{g1}\, Z(\theta, \lambda)^{-c_{g2}} = c_{g1} \left[\lambda\, \exp\left(\frac{E^*}{R\,\theta}\right)\right]^{-c_{g2}} \leq d_g, \tag{14}$$

where c_{g1} and c_{g2} are the steady state average grain size material parameters and Z is the Zener-Hollomon parameter [22]. The steady state average grain size increases with increasing temperature, which is in agreement with experimental results. For static annealing processes, the average grain size reduction rate vanishes and an average grain size growth is predicted. Under cold working conditions, the grain size remains constant.

3 | THERMODYNAMICAL CONSISTENCY

The proposed hyper-elasticity based thermoplasticity framework enables the investigation of thermodynamical consistency for the underlying unified constitutive recrystallisation model by considering the reduced mechanical dissipation inequality introduced in (5). Inserting the associated evolution equation of plastic flow, (7), and the non-associated evolution equation of the proportional hardening related internal variable, (9), results in

$$\mathcal{D}^{\text{red}}_{\text{mech}} = \lambda \left[\sqrt{\frac{3}{2}} \|\boldsymbol{m}^{\text{tdev}}\| - \left[1 - X\right] \left[\frac{d_{g0}}{d_g}\right]^z \beta\right] + \left[\sqrt{\frac{2}{3}}\, R_d(\theta)\, \lambda + R_s(\theta)\right] \frac{\beta^2}{H(\theta)} \left[\frac{d_{g0}}{d_g}\right]^z \beta \geq 0. \tag{15}$$

In the case of static annealing, plastic loading is not active and $\lambda = 0$. Inserting this condition into the above inequality results in the static contribution to the reduced mechanical dissipation inequality in the form

$$\mathcal{D}^{\text{red}}_{\text{mechs}} = R_{\text{s}}(\theta)\,\frac{\beta^2}{H(\theta)}\left[\frac{d_{\text{g0}}}{d_{\text{g}}}\right]^{z}\beta \geq 0\,. \tag{16}$$

Since R_{s}, H, d_{g0}, d_{g} and β are all non-negative quantities, thermodynamical consistency for static annealing processes is confirmed. For hot working processes with $\lambda > 0$, the initial form of (15) reduces to the dynamic contribution to the reduced mechanical dissipation inequality of the form

$$\mathcal{D}^{\text{red}}_{\text{mechd}} = \lambda\left[\sqrt{\frac{3}{2}}\|\boldsymbol{m}^{\text{tdev}}\| - [1-X]\left[\frac{d_{\text{g0}}}{d_{\text{g}}}\right]^{z}\beta\right] \geq 0\,, \tag{17}$$

where the second term in (15) was assumed to be positive by employing the same arguments of positive functions as before and, in consequence, is neglected in (17). Introducing the abbreviating notation of $y := [1-X]\,[d_{\text{g0}}/d_{\text{g}}]^{z}$, together with assuming $y \leq 1$ and inserting the yield criterion $\Phi = 0$, cf. (6), into the above inequality results in

$$\mathcal{D}^{\text{red}}_{\text{mechd}} = \lambda\left[\sqrt{\frac{3}{2}}\|\boldsymbol{m}^{\text{tdev}}\| - y\,\beta\right] \geq \lambda\left[\sqrt{\frac{3}{2}}\|\boldsymbol{m}^{\text{tdev}}\| - \beta\right] = \lambda\,\sigma_{y0}(\theta) \geq 0\,, \tag{18}$$

such that thermodynamical consistency is confirmed for hot working processes if the condition $y \leq 1$ holds. Therefore, thermodynamical consistency is directly obtained for grain size growth controlled hot working processes. For grain size reduction controlled hot working processes, due to $[d_{\text{g0}}/d_{\text{g}}]^{z} \geq 1$, thermodynamical consistency must be verified manually in terms of showing that $y \leq 1$ which gives rise to the thermodynamical intercorrelation between the internal variables of recrystallised volume fraction and average grain size. Note that thermodynamical consistency can still be achieved even if the condition $y \leq 1$ is violated, due the second term in (15) including R_{d} and R_{s} potentially compensating negative values of $\mathcal{D}^{\text{red}}_{\text{mechd}}$ in (17). If thermodynamical consistency is obtained, the resulting reduced mechanical dissipations of the form (15) and (16) can be considered as a heat source in hot working and static annealing processes, respectively, which is motivated by the release of hardening related energy contributions.

4 | NUMERICAL EXAMPLES

Based on the proposed hyper-elasticity based recrystallisation formulation and the derived constraint condition for grain size refinement controlled hot working processes, thermodynamical consistency can be verified by analysing representative thermomechanical sequential loading conditions including static annealing and hot working. An algorithmic formulation of the underlying model is obtained by employing an implicit backward Euler time integration for the evolutions of the proportional hardening variable, recrystallised volume fraction and average grain size. For the evolution of the plastic deformation gradient, an implicit exponential time integration scheme is applied that preserves plastic incompressibility and an initial recrystallised volume fraction of $X = 10^{-6}$ is adopted to ensure numerical stability, cf. (11). For static annealing processes, the coupling between recrystallisation and the proportional hardening rate is achieved by introducing a modified backward Euler time integration scheme, as proposed by Cho et al. [5], of type $\alpha_{n+1} = [1-X_{n+1}]/[1-X_n]\,\alpha_n + \Delta t\,\dot{\alpha}_{n+1}$ if $\Delta X = X_{n+1} - X_n > 0$. This formulation accounts for the consumption of original grains during recrystallisation. The resulting effect under hot working conditions on thermodynamical consistency remains for future work.

Figure 1 shows the results obtained for a sequential load-unload-hold test using the material parameters listed in Table 1. During a first hot working step, homogeneous states of deformation under uniaxial tension are enforced, followed by an unloading and holding at various temperatures in a second step. The deformation gradient takes the form $\boldsymbol{F} = \lambda_{\|}\,\boldsymbol{e}_{\|} \otimes \boldsymbol{e}_{\|} + \lambda_{\perp}[\boldsymbol{I} - \boldsymbol{e}_{\|} \otimes \boldsymbol{e}_{\|}]$ such that a uniaxial tension stress state $\boldsymbol{\sigma} = \sigma_{\|}\,\boldsymbol{e}_{\|} \otimes \boldsymbol{e}_{\|}$ is obtained. The results show a softening effect in the evolution of the hardening stress, see Figure 1A, a sigmoidal evolution of recrystallised volume fraction, see Figure 1B, a grain size reduction followed by grain size growth in Figure 1C and ultimately a thermodynamical consistent

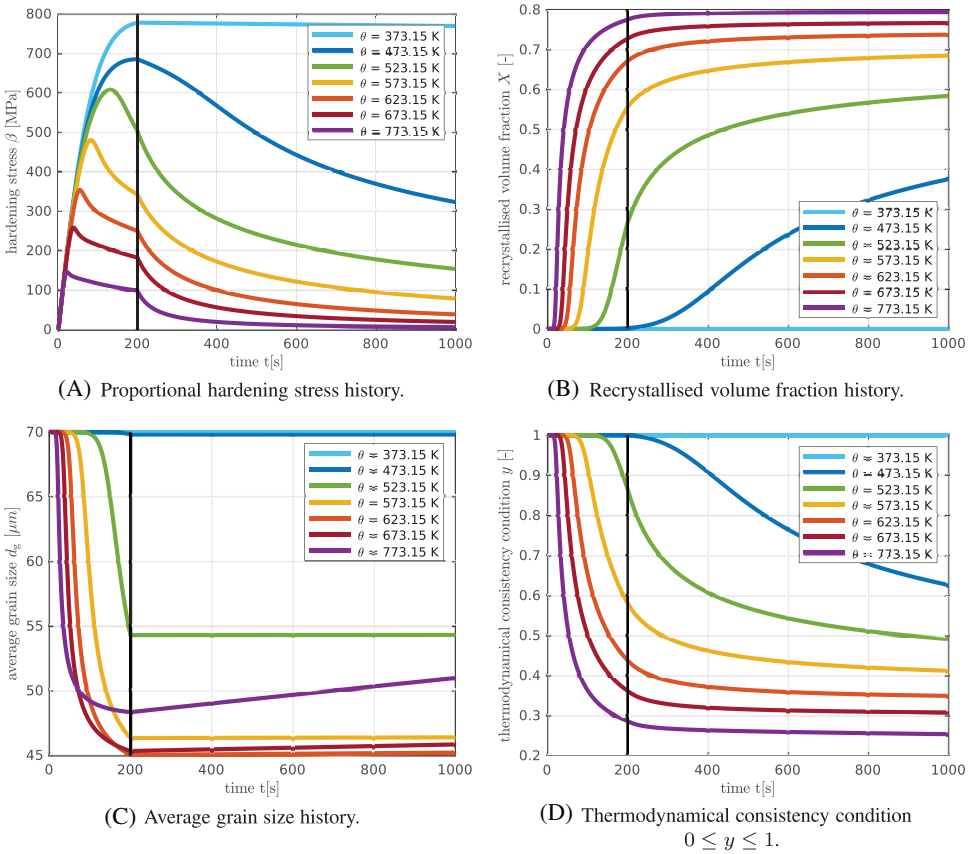

(A) Proportional hardening stress history.

(B) Recrystallised volume fraction history.

(C) Average grain size history.

(D) Thermodynamical consistency condition $0 \leq y \leq 1$.

FIGURE 1 Thermomechanical sequential load-unload-hold test for grain size refinement controlled hot working processes.

TABLE 1 Material parameters slightly modified from those provided by Cho et al. [5] for copper (K, G, H, σ_{y0} are set constant).

K_0	135.417 GPa	C_{13}	5.098×10^{-2} 1/MPa	c_{x1}	1.780×10^{6} 1/MPa	c_{g1}	7.410×10^{2} µm s$^{-c_{g2}}$	a	8.052×10^{-1}
G_0	48.508 GPa	C_{14}	3.963×10^{3} J/mol	c_{x2}	6.490×10^{4} J/mol	c_{g2}	8.826×10^{-1}	b	3.680×10^{0}
$\bar{c}_0/\varrho_0$	0.385 J/[g K]	C_{17}	2.487×10^{0} 1/[MPa s]	c_{x3}	5.401×10^{4} 1/[MPa s]	c_{g3}	1.185×10^{-3} 1/µm^2	c	4.485×10^{0}
H_0	8000.0 MPa	C_{18}	6.328×10^{4} J/mol	c_{x4}	7.436×10^{4} J/mol	ω_0	8.600×10^{4} µm^n/s	z	0.650×10^{0}
σ_{y0}	200.0 MPa	ϱ_0	8.96 g/cm^3	c_{x5}	5.000×10^{0}	E^*	8.200×10^{4} kJ/mol	n	2.000×10^{0}

response, where the thermodynamical consistency condition is fulfilled during the grain size refinement controlled hot working process, see Figure 1D.

5 | SUMMARY AND OUTLOOK

The hyper-elasticity based formulation proposed in this work, which builds upon the hypo-elasticity based model by Cho et al. [5], allows for the derivation of a thermodynamical consistency condition. It is shown that this condition effectively constrains the evolution of internal variables, namely the recrystallised dislocation-free volume fraction and average grain size, and gives rise to the thermodynamical intercorrelation between them. When applied to static annealing and grain size growth controlled hot working processes, the model produces thermodynamically consistent and physically sound results, adhering to the second law of thermodynamics. The thermodynamical consistency condition is further investigated under thermomechanical sequential loading conditions for grain size refinement controlled hot working processes. The results demonstrate the capability of the proposed model to thermodynamically accurately predict the microstructural evolution, including the associated recrystallisation effects. The fundamental developments presented in this contribution provide a basis for future research, including potential extensions such as incorporating a Perzyna type ansatz [23] to account for

strain rate dependency in the plasticity formulation. In addition, the current framework is to be extended to include a damage formulation [24], where ensuring thermodynamic consistency within the framework will be crucial, particularly when modelling self-healing during recrystallisation.

ACKNOWLEDGMENTS

Financial support by the Deutsche Forschungsgemeinschaft (DFG, German Research Foundation), Project-ID 278868966, TRR 188, is gratefully acknowledged.

Open access funding enabled and organized by Projekt DEAL.

ORCID

Merlin Böddecker https://orcid.org/0000-0002-6759-7230
Andreas Menzel https://orcid.org/0000-0002-7819-9254

REFERENCES

1. Doherty, R. D., Hughes, D. A., Humphreys, F. J., Jonas, J. J., Jensen, D. J., Kassner, M. E., King, W. E., McNelley, T. R., McQueen, H. J., & Rollett, A. D. (1997). Current issues in recrystallization: A review. *Materials Science and Engineering A*, *238*(2), 219–274.
2. Humphreys, J., Rohrer, G. S., & Rollett, A. (2017). *Recrystallization and related annealing phenomena*. Elsevier.
3. Hall, E. O. (1951). The deformation and ageing of mild steel: III discussion of results. *Proceedings of the Physical Society, Section B*, *64*(9), 747–755.
4. Petch, N. J. (1953). The cleavage strength of polycrystals. *Journal of the Iron and Steel Institute*, *174*(1), 25–28.
5. Cho, H. E., Hammi, Y., Bowman, A. L., Karato, S., Baumgardner, J. R., & Horstemeyer, M. F. (2019). A unified static and dynamic recrystallization Internal State Variable (ISV) constitutive model coupled with grain size evolution for metals and mineral aggregates. *International Journal of Plasticity*, *112*, 123–157.
6. Guillope, M., & Poirier, J. P. (1979). Dynamic recrystallization during creep of single-crystalline halite: An experimental study. *Journal of Geophysical Research*, *84*(B10), 5557–5567.
7. Sellars, C. M. (1978). Recrystallization of metals during hot deformation. *Philosophical Transactions of the Royal Society of London. Series A*, *288*, 147–158.
8. Raabe, D. (2007). A texture-component avrami model for predicting recrystallization textures, kinetics and grain size. *Modelling and Simulation in Materials Science and Engineering*, *15*(2), 39–63.
9. Zurob, H. S., Brechet, Y., & Purdy, G. (2001). A model for the competition of precipitation and recrystallization in deformed austenite. *Acta Materialia*, *49*(20), 4183–4190.
10. Bacca, M., Hayhurst, D. R., & McMeeking, R. M. (2015). Continuous dynamic recrystallization during severe plastic deformation. *Mechanics of Materials*, *90*, 148–156.
11. Cram, D. G., Zurob, H. S., Brechet, Y. J. M., & Hutchinson, C. R. (2009). Modelling discontinuous dynamic recrystallization using a physically based model for nucleation. *Acta Materialia*, *57*(17), 5218–5228.
12. Kugler, G., & Turk, R. (2004). Modeling the dynamic recrystallization under multi-stage hot deformation. *Acta Materialia*, *52*(15), 4659–4668.
13. Liu, J., Cui, Z., & Ruan, L. (2011). A new kinetics model of dynamic recrystallization for magnesium alloy AZ31B. *Materials Science and Engineering A*, *529*, 300–310.
14. Avrami, M. (1939). Kinetics of phase change. I general theory. *Journal of Chemical Physics*, *7*, 1103–1112.
15. Avrami, M. (1940). Kinetics of phase change. II transformation time relations for random distribution of nuclei. *Journal of Chemical Physics*, *8*, 212–224.
16. Brown, A. A., & Bammann, D. J. (2012). Validation of a model for static and dynamic recrystallization in metals. *International Journal of Plasticity*, *32–33*, 17–35.
17. Busso, E. P. (1998). A continuum theory for dynamic recrystallization with microstructure-related length scales. *International Journal of Plasticity*, *14*(4-5), 319–353.
18. Roucoules, C., Pietrzyk, M., & Hodgson, P. D. (2003). Analysis of work hardening and recrystallization during the hot working of steel using a statistically based internal variable model. *Materials Science and Engineering A*, *339*(1-2), 1–9.
19. Armstrong, P. J., & Frederick, C. O. (1966). A mathematical representation of the multiaxial bauschinger effect. Berkeley Nuclear Laboratories, Central Electricity Generating Board Report RD/B/N 731.
20. Hencky, H. (1928). Über die form des elastizitätsgesetzes bei ideal elastischen stoffen. Zeitschrift für Technische Physik, *9*, 214–247.
21. Coleman, B. D., & Noll, W. (1963). The thermodynamics of elastic materials with heat conduction and viscosity. *Archive for Rational Mechanics and Analysis*, *13*(1), 167–178.
22. Zener, C., & Hollomon, J. H. (1944). Effect of strain rate upon plastic flow of steel. *Journal of Applied Physics*, *15*, 22–32.
23. Oppermann, P., Denzer, R., & Menzel, A. (2022). A thermo-viscoplasticity model for metals over wide temperature ranges- application to case hardening steel. *Computational Mechanics*, *69*(2), 541–563.

24. Sprave, L., & Menzel, A. (2020). A large strain gradient-enhanced ductile damage model: Finite element formulation, experiment and parameter identification. *Acta Mechanica*, *231*(12), 5159–5192.

How to cite this article: Böddecker, M., & Menzel, A. (2023). A large strain thermoplasticity model including recovery, recrystallisation and grain size effects. *Proceedings in Applied Mathematics and Mechanics*, *23,* e202300282. https://doi.org/10.1002/pamm.202300282